JOURNAL OF APPLIED ELECTROCHEMISTRY 22 (1992) 657–662

Electrodeposition of zinc–nickel alloy coatings from a chloride bath containing NH_4Cl

R. FRATESI, G. ROVENTI

Dipartimento di Scienze dei Materiali e della Terra, Università di Ancona. Via Brecce Bianche, 60131 Ancona, Italy

Received 4 June 1991; revised 10 October 1991

Zinc–nickel alloys were electrodeposited on steel from chloride baths containing NH_4Cl using different plating conditions. Current density, temperature and nickel percentage in the baths were found to strongly influence the composition of the deposits and the morphology. At low current densities transition from anomalous to normal codeposition was observed. The changes in potential, current efficiency, composition and morphology which follow the transition were studied. No increase in the partial current of hydrogen reduction was observed at the potential values from which anomalous codeposition begins; this fact, plus the formation of zinc ammonium complexes, seems to exclude the precipitation of zinc hydroxide at the electrode surface. The electrodeposition of zinc–nickel alloys is discussed emphasizing the importance of kinetic parameters and cathodic potentials.

1. Introduction

In the past decade many efforts have been made to develop high corrosion-resistant steel sheets especially for automotive body panels [1–4]. Recently, it has been shown that electrodeposited zinc–iron group metal alloys are suitable materials for this application [1–8]. A major development in this area has focused on zinc–nickel alloy coatings, which show remarkable corrosion resistance after the chromating process [9–11]. These electrodeposits also lead to a low hydrogen embrittlement on the metal substrate, so they have been proposed as a suitable substitute for cadmium coatings [12].

The electrodeposition of zinc–nickel alloys is a codeposition of anomalous type according to the Brenner definition [13], that is the less noble metal deposits preferably on the cathode with respect to the more noble one. The operating conditions such as current density, temperature, pH, organic additives, buffer capacity, concentration of all solution components, etc. lead to changes in the kinetics of electrodeposition, composition and morphology of the coatings, as well as in their physico-mechanical characteristics [14–19]. So, it is possible to obtain normal codeposition even in particular electrodeposition conditions.

Since the galvanic industries use baths containing NH_4Cl to deposit zinc–nickel alloys, we have likewise electrodeposited this alloy from similar baths containing different metal ion concentrations. The influence of different parameters (temperature, bath composition, current density) on the transition current, phase and morphology modification of the alloys obtained has also been studied.

2. Experimental details

Zinc–nickel alloys were obtained at 40 $\pm$ 1 °C, under galvanostatic conditions, using baths of the following composition: 28.7 to 67.2 g dm^{-3} $NiCl_2 \cdot 6H_2O$ (0.12 to 0.28 M Ni^{2+}), 20.7 to 8.8 g dm^{-3} ZnO (0.25 to 0.11 M Zn^{2+}), 125 to 250 g dm^{-3} NH_4Cl, 20 g dm^{-3} H_3BO_3, 0.5 g dm^{-3} dodecyldiethoxy sodium sulphate, 1 g dm^{-3} gelatine; pH 5.8. Some deposits were obtained from baths whose pH was lowered to 4.6 on addition of HCl; it was impossible to work at a lower pH because the large quantity of HCl would have precipitated the salts present in the solution.

Solutions were prepared with doubly distilled water and analytical grade reagents. To investigate the influence of temperature on the deposits composition, some electrodepositions were carried out at 30 and 54 °C. A PVC cell 1 dm^3 in capacity was used. Electrodeposits were obtained on both sides of mild steel discs, 1 mm thick (exposed area 15 cm^2), which were fixed on a mobile frame, kept in oscillating motion.

Before electrodeposition, the samples were smoothed with emery paper; then any grease was removed from their surface by anodic and cathodic electrolysis for 2 min in an aqueous NaOH 60 g dm^{-3} solution at 4 V against graphite anodes. The samples were then neutralized in a 2% HCl solution and rinsed with distilled water.

The anodes were zinc (total area 500 cm^2) and nickel (total area 100 cm^2) sheets; the anodic dissolution was regulated by two separate circuits, fed by two galvanostats, where 83% of the total current intensity passed through the zinc anodes and 17% passed through the nickel ones. In this way, zinc and nickel

0021-891X/92

consumption due to their reduction at the cathode was compensated. Before immersion in the bath, the zinc anodes were immersed for 3 h, without current flow, in a solution of similar composition at 40 °C. The zinc sheets were coated with a dark nickel layer, so avoiding the depletion of nickel in the bath due to its cementation on the zinc anodes.

Cathode potential measurement was performed during electrodeposition using a Ag/AgCl reference electrode. Polarization was applied when the cathode was immersed in the bath and electrolysis was continued until deposits 6 μm thick were obtained. The disc cathodes were thoroughly washed with water and then ethanol, hot air dried and weighed.

To determine the percentage composition of the electrodeposited alloys, the deposits were stripped in a minimum volume of 1 : 3 HCl solution and analysed for nickel and zinc by means of inductively coupled plasma spectroscopy (ICPS). By means of Faraday's law, the partial currents of zinc and nickel were calculated and their respective polarization curves were plotted.

The morphology of the deposits was observed by means of scanning electron microscopy (SEM). The deposited phases were analysed by the X-ray diffraction method by CuK_α (λ = 15.4 nm) and identified by powder diffraction file card (JCPDS).

All the tests were repeated three times with good agreement.

3. Results and discussion

3.1. *Effect of operating variables on the nickel percentage in the coatings*

Coherent and homogeneous coatings were obtained with current density up to 100 mA cm^{-2}. Above this value, the deposits appeared less uniform and dendritic growth was observed along the edges of the samples. Text figures, however, for simplicity, show results obtained up to 50 mA cm^{-2}.

The effects of the nickel ion percentage in the bath, temperature, NH_4Cl concentration and pH on the percentage composition of the deposits were studied. It was observed that the percentage of nickel in the alloys was approximately constant over a wide current density range and increased strongly at the lowest current density values (Figs 1 and 2). Temperature and percentage of nickel ions in the bath strongly affected the composition of the deposits, while a decrease in pH and concentration of NH_4Cl did not markedly affect the general trend shown in Figs 1 and 2, causing only a slight decrease in the nickel percentage in the deposit.

With the operating conditions used, the transition from anomalous to normal codeposition occurs at the points indicated by the letters A, B and C in Fig. 1 and at the intersecting points of the composition reference line (CRL) with the curves obtained at different temperatures in Fig. 2.

The transition current density (i_T) as a function of

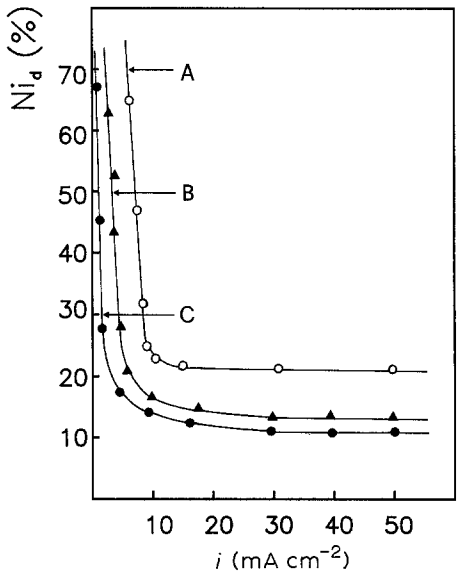

Fig. 1. Effect of current density on the percentage of nickel in zinc–nickel alloys electrodeposited from baths containing the following percentages of nickel: (○) 70%, (▲) 50%, (●) 30%. A, B, C indicate the points where the transition from normal to anomalous codeposition occurs. T = 40 °C, NH_4Cl = 250 g dm^{-3}, pH 5.8.

the parameters characteristic of the bath (pH, percentage of nickel, temperature and NH_4Cl concentration) is shown in Fig. 3. The temperature strongly influences i_T, while other parameters have less effect. The transition current density does not depend on the total metal quantity contained in the bath, where the total metal is the sum of the Zn^{2+} and Ni^{2+} ions.

The effect of current density on alloy composition, on current efficiencies of the alloy deposition and of the hydrogen reduction, together with the polarization curve are shown in Fig. 4. In correspondence with the transition current density, there is a sharp decrease in the potential and current efficiency in the alloy deposition, and an increase in the current efficiency of

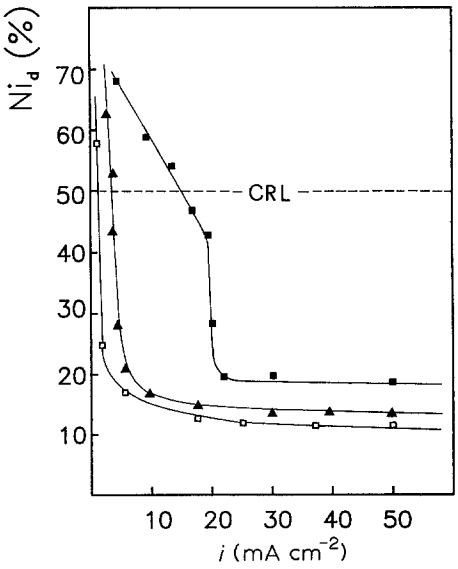

Fig. 2. Effect of current density on the percentage of nickel in zinc–nickel alloys electrodeposited at the following temperatures: (■) 54 °C, (▲) 40 °C, (□) 30 °C. CRL: Composition Reference Line. Ni$_b$ = 50%, NH_4Cl = 250 g dm^{-3}, pH 5.8.

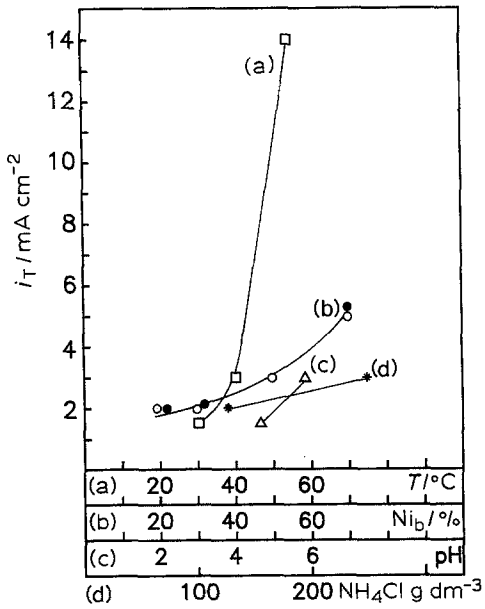

Fig. 3. Effect of temperature (a), nickel percentage in the bath (b), pH (c) and NH_4Cl concentration (d) on the transition current density. (a) Ni_b = 50%, NH_4Cl = 250 g dm^{-3}, pH 5.8; (b) (○) M_{tot} = 23.7 g dm^{-3}, (●) M_{tot} = 33.2 g dm^{-3}. NH_4Cl = 250 g dm^{-3}, pH 5.8, T = 40 °C, (c) Ni_b = 50%, NH_4Cl = 250 g dm^{-3}, T = 40 °C; and (d) Ni_b = 50%, pH 5.8, T = 40 °C.

hydrogen reduction. This pattern was confirmed by all the measurements carried out in the present work and has also been found by other authors [17].

Recently, Higashi *et al.* [14] and Fukushima *et al.* [17] have re-proposed the Dahms and Croll theory [20] for the anomalous codeposition of Zn–Co and Zn–Ni alloys, respectively, from sulphate baths. The anomalous behaviour is attributed to the formation of a zinc hydroxide film on the electrode surface, which suppresses the discharge of nickel or cobalt ions. The zinc hydroxide formation arises from the local increase in pH due to the hydrogen reduction.

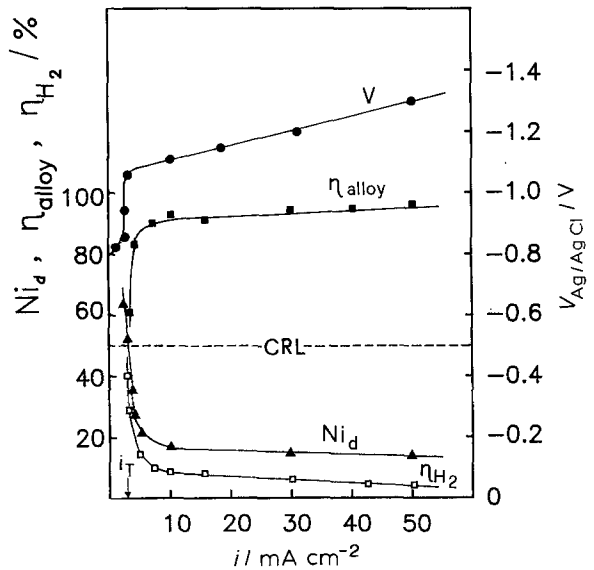

Fig. 4. Polarization curve during alloy deposition (V) and effect of current density on nickel content of deposits (Ni_d), on current efficiency for alloy deposition (η_{alloy}) and on current efficiency for hydrogen reduction (η_{H_2}). Ni_b = 50%, NH_4Cl = 250 g dm^{-3}, pH 5.8, T = 40 °C.

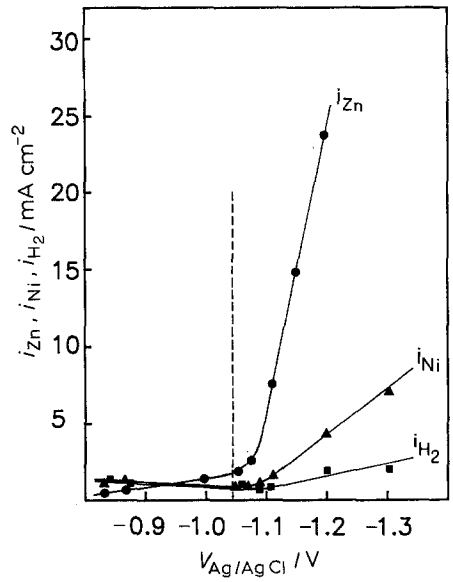

Fig. 5. Polarization curves for zinc, nickel and hydrogen reduction. Ni_b = 50%, NH_4Cl = 250 g dm^{-3}, pH 5.8, T = 40 °C.

The partial currents of zinc, nickel and hydrogen as a function of the electrolysis potential are reported in Fig. 5. The vertical line sketched indicates the potential value from which normal deposition begins. In the immediate vicinity of this potential no increase in the hydrogen partial current is observed.

Furthermore, the presence of NH_4Cl in the bath and stirring during electrolysis prevent precipitation of zinc hydroxide. In Fig. 6, the pH values obtained on successive additions of NaOH 10 M to the electrodeposition bath and to a similar solution containing only $ZnCl_2$ and $NiCl_2 \cdot 6H_2O$ at pH 3.3 are reported. As NaOH is added, the bath progressively changes colour, from greenish-blue to blue and NH_3 is evolved. This suggests the formation of ammonium complexes, such as $[Zn(NH_3)_4]^{2+}$ and $[Ni(NH_3)_6]^{2+}$ (blue colour), which prevent hydroxide precipitation that starts at point A. In the solution without NH_4Cl, precipitation

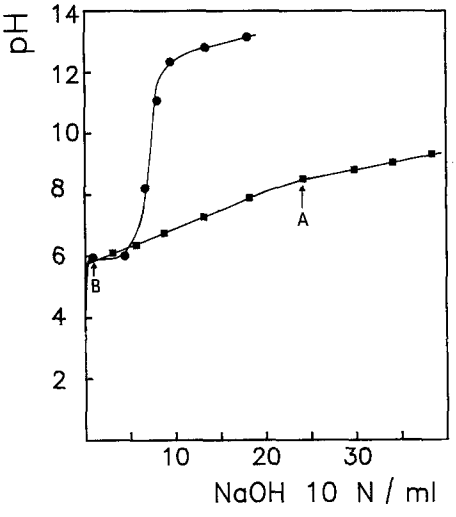

Fig. 6. Effect of successive additions of 10 N NaOH on the pH of the bath (■) and on the pH of a solution containing $ZnCl_2$ and $NiCl_2 \cdot 6H_2O$ at equal concentration (●). Titrated volume 100 cm^3. A and B indicate the points where the zinc hydroxide precipitation starts.

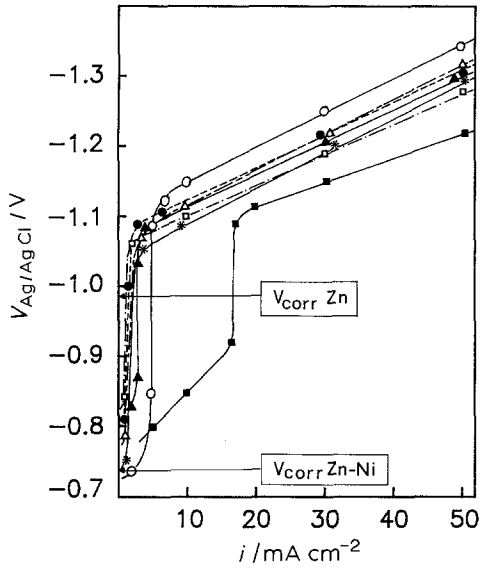

Fig. 7. Polarization curves of zinc–nickel alloys electrodeposition at different experimental conditions: (○) Ni_b = 70%, NH_4Cl = 250 g dm^{-3}, pH 5.8, T = 40 °C; (▲) Ni_b = 50%, NH_4Cl = 250 g dm^{-3}, pH 5.8, T = 40 °C; (●) Ni_b = 30%, NH_4Cl = 250 g dm^{-3}, pH 5.8, T = 40 °C; (△) Ni_b = 50%, NH_4Cl = 125 g dm^{-3}, pH 5.8, T = 40 °C; (*) Ni_b = 50%, NH_4Cl = 250 g dm^{-3}, pH 4.6, T = 40 °C; (■) Ni_b = 50%, NH_4Cl = 250 g dm^{-3}, pH 5.8, T = 54 °C; (□) Ni_b = 50%, NH_4Cl = 250 g dm^{-3}, pH 5.8, T = 30 °C.

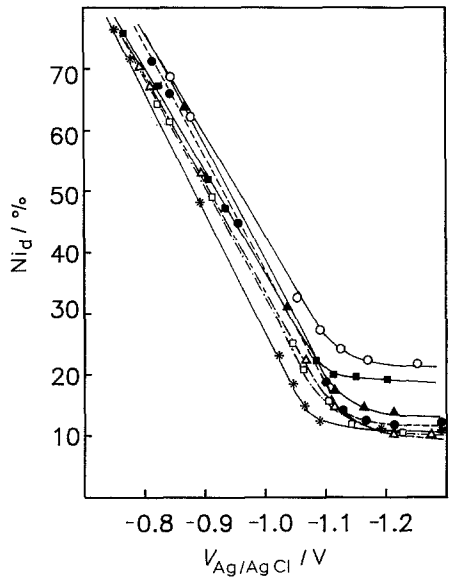

Fig. 8. Effect of cathodic potentials of electrolysis on the nickel percentage of electrodeposits. Symbols for different experimental conditions as for Fig. 7.

of zinc hydroxide occurs as soon as NaOH is added and the pH remains constant until precipitation ends.

These results suggest that, with the experimental conditions used in this work, the Dahms and Croll theory is not confirmed.

Previously [15, 21], even for different bath conditions, anomalous codeposition of Zn–Co and Zn–Ni alloys has been treated, emphasizing the importance of the kinetic parameters of the cathodic reactions. The iron group metals are generally characterized by very low exchange current densities, unlike zinc, which shows high exchange current density. Furthermore, it is evident from Fig. 3 that the transition current increases with increase in bath temperature, confirming the key role played by the temperature dependent kinetic parameters.

This hypothesis is also supported by Mathias *et al.* [22, 23] who, using the Roehl bath (pH 1.6), found that the electrodeposition of zinc–nickel alloys is anomalous even though the hydrogen current is not high enough to raise the interfacial pH much above the bulk pH, as would be necessary for formation of zinc hydroxide. These authors calculated that the zinc exchange current density is five orders of magnitude higher than that of the nickel and attributed the anomalous codeposition to the intrinsically slow nickel kinetics.

In Fig. 7 the potential/current density curves obtained under all the different experimental conditions are shown. When codeposition of normal type occurs, the cathodic potentials reach values close to the free corrosion potential of zinc (−995 mV against Ag/AgCl) and of zinc–nickel alloys (−740 mV against Ag/AgCl for alloys containing 12–14% Ni). Both materials undergo considerable corrosion during immersion in the bath, with preferential dissolution of zinc in zinc–nickel deposits. This suggests that the potential at which codeposition occurs is probably not sufficiently negative to assure zinc reduction, so causing a contemporary and partial dissolution of the metal already deposited. This hypothesis is also supported by the fact that the current efficiencies of the alloys during normal codeposition are always very low. A further confirmation comes from Fig. 8 where the percentage of nickel in the deposits for all the different experimental conditions used, as a function of the relative potentials of deposition, is given. The composition percentage of the deposits obtained depends mainly on the potential of electrolysis.

3.2. *Appearance and microstructure of the electrodeposits*

By diffractometric analysis and scanning electron

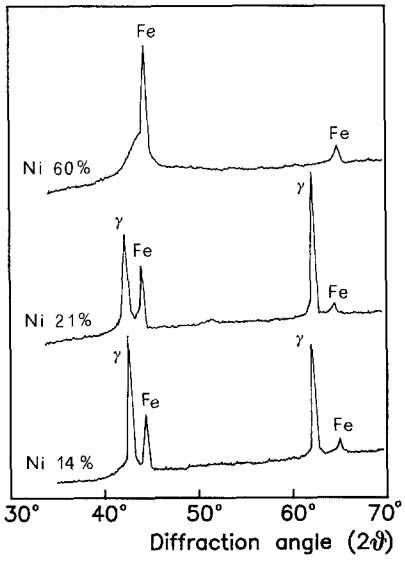

Fig. 9. X-ray diffraction profiles of electrodeposits containing different percentages of nickel.

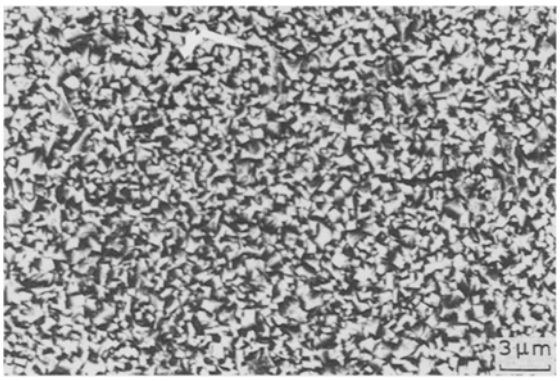

Fig. 10. Microstructure of zinc-nickel alloys containing 14% nickel.

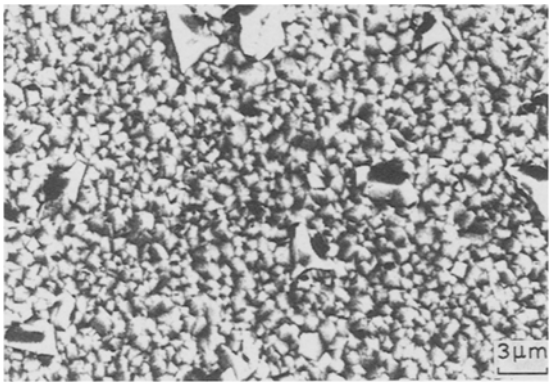

Fig. 11. Microstructure of zinc–nickel alloys containing 21% of nickel.

microscopy, the presence of different phases in the electrodeposits and their surface morphology was studied. The type of phases and the morphology depend on the percentage of nickel in the deposits, once the addition agents are constant.

Diffractometric X-rays of the deposits containing different percentages of nickel, are shown in Fig. 9. Only the γ phase (Ni_5Zn_{21}) is present in coatings with over 8–9% Ni [15, 16]. Increasing the nickel content up to 25–30%, the γ phase remains the only one present, but the $2\theta = 62.2°$ peak prevails, which corresponds to a variation in the growth of the grains.

When the electrolysis current is lower than the transition current and the nickel content is greater than 50%, the γ phase disappears: from the diffractogramme only the peaks relative to the ferrous substrate can be seen and the coating is amorphous.

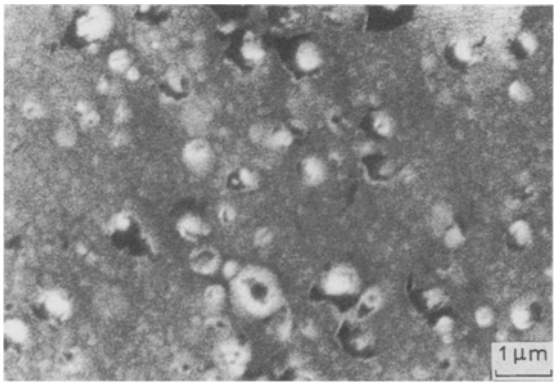

Fig. 12. Microstructure of zinc–nickel alloys containing 60% nickel.

Concomitant changes in structure can be observed by SEM analysis. In Figs 10, 11 and 12 microstructures of deposits containing 14, 21 and 60% Ni, respectively, are shown. Alloys with 14% Ni show a homogeneous structure formed of crystallites with columnar growth of pyramidal form; those with 21% Ni still show a pyramidal columnar structure, slightly finer, homogeneous and with emerging crystallites of greater dimensions. The morphological structure of deposits containing 60% Ni is completely different. They are not crystalline, but flat, with some heterogeneities, confirming diffractometric analysis.

4. Conclusions

Zinc–nickel alloys with satisfactory physical and mechanical properties were electrodeposited from chloride baths containing NH_4Cl. The alloy composition and morphology depend mainly on the temperature, current density and nickel percentage in the baths, with the addition agents constant.

At low current density transition from anomalous to normal codeposition occurs. The nickel percentage of the deposit becomes higher than that present in the bath, the current efficiency of the alloy decreases and the cathodic potential shifts towards more positive values. At the transition current density, no increase in hydrogen evolution was found.

The anomalous codeposition of zinc–nickel alloys is attributed to the intrinsically slow nickel kinetics.

Normal codeposition occurs at potentials close to the free corrosion potential of zinc and of zinc–nickel alloys and with very low current efficiency. This, and the fact that the nickel percentage of the alloys depend mainly on the potential of electrolysis, suggests that the potential at which normal codeposition occurs is probably not sufficiently negative to assure zinc reduction, causing partial dissolution of the metal already deposited.

Acknowledgements

The research was supported by the National Research Council of Italy.

References

[1] T. Watanabe, M. Omura, T. Honma and T. Adaniya, *SAE Tech. Pap. Series No 820424*, Detroit, Michigan (1982).
[2] A. Shibuya, T. Kurimoto, K. Korekawa and K. Noji, *Tetsu to Hagane* **66** (1980) 771.
[3] R. Noumi, H. Nagasaki, Y. Foboh and A. Shibuya, *SAE Tech. Pap. Series No 820332*, Detroit, Michigan (1982).
[4] T. Kurimoto, Y. Foboh, H. Oishi, K. Yanagawa and R. Noumi, *SAE Tech. Pap. Series No 831837*, Warrendale, Pennsylvania (1983).
[5] K. Ariga and K. Kanda, *Tetsu to Hagane* **66** (1980) 797.
[6] T. Fukuzuka, K. Jajiawara and K. Miki, *ibid.* **66** (1980) 807.
[7] V. Raman, M. Pushpavanam, S. Jayakrishnan and B. A. Shenoi, *Met. Finish.* **81**(1983) 85.
[8] D. E. Hall, *Plat. Surf. Finish.* **71** (1983) 59.
[9] M. R. Lambert, R. G. Hart and H. E. Townsend, *SAE Tech. Pap. Series No 831817*, Warrendale, Pennsylvania (1983).

[10] L. Felloni, R. Fratesi, G. Roventi and L. Fedrizzi, Proceedings of the 11th International Corrosion Congress, Vol. 2, Florence, Italy, (26 April 1990) p. 365.
[11] L. Fedrizzi, R. Fratesi, L. Ciaghi, G. Roventi and P. L. Bonora, *J. Appl. Electrochem.*, in press.
[12] G. F. Hsu, *Plat. Surf. Finish.* **71** (1984) 52.
[13] A. Brenner, 'Electrodeposition of alloys' Vols I and II, Academic Press, New York and London (1963).
[14] K. Higashi, H. Fukushima, T. Urokawa, T. Adaniya and K. Matsudo, *J. Electrochem. Soc.* **128** (1981) 2081.
[15] L. Felloni, R. Fratesi, E. Quadrini and G. Roventi, *J. Appl. Electrochem.* **17** (1987) 574.
[16] L. Felloni, R. Fratesi and G. Roventi, Proceedings of the XXII International Metals Congress, Bologna, Italy, (17–19 May 1988) p. 687.
[17] H. Fukushima, T. Akiyama, K. Higashi, R. Kammel and M. Karimkhani, *Metall.* **42** (1988) 242.
[18] R. Albalat, E. Gomez, C. Muller, M. Sarret, E. Vallés and J. Pregonas, *J. Appl. Electrochem.* **20** (1989) 529.
[19] R. Albalat, E. Gomez, C. Muller, M. Sarret, E. Vallés and J. Pregonas, *ibid.* **20** (1990) 635.
[20] H. Dahms and I. M. Croll, *J. Electrochem. Soc.* **112** (1965) 771.
[21] R. Fratesi and G. Roventi, *Mater. Chem. Phys.* **23** (1989) 529.
[22] M. F. Mathias and T. W. Chapman, *J. Electrochem. Soc.* **134** (1987) 1408.
[23] M. F. Mathias and T. W. Chapman, *J. Electrochem. Soc.* **137** (1990) 102.